



Published in final edited form as:

*J Neurosci.* 2008 July 9; 28(28): 7104–7112. doi:10.1523/JNEUROSCI.0378-08.2008.

## Behavioral impact of neurotransmitter-activated GPCRs: Muscarinic and GABA<sub>B</sub> receptors regulate *C. elegans* locomotion

Jeremy S Dittman and Joshua M Kaplan

Department of Molecular Biology, Massachusetts General Hospital, Boston MA, 02114

### Abstract

Neurotransmitter released from presynaptic terminals activates both ligand-gated ion channels (ionotropic receptors) and a variety of G protein-coupled receptors (GPCRs). These neurotransmitter receptors are expressed on both pre- and postsynaptic cells. Thus, each neurotransmitter acts on multiple receptor classes, generating a large repertoire of physiological responses. The impact of many ionotropic receptors on neuronal activity and behavior has been clearly elucidated; however, much less is known about how neurotransmitter-gated GPCRs regulate neurons and circuits. In *C. elegans*, both Acetylcholine (ACh) and GABA are released in the nerve cord and mediate fast neuromuscular excitation and inhibition during locomotion. Here we identify a muscarinic receptor (GAR-2) and the GABA<sub>B</sub> receptor dimer (GGB-1/2) that detect synaptically released ACh and GABA, respectively. Both GAR-2 and GGB-1/2 inhibited cholinergic motor neurons when ACh and GABA levels were enhanced. Loss of either GPCR resulted in movement defects, suggesting that these receptors are activated during locomotion. When the negative feedback provided by GAR-2 was replaced with positive feedback, animals became highly sensitive to ACh levels and locomotion was severely impaired. Thus, conserved GPCRs act in the nematode motor circuit to provide negative feedback and to regulate locomotory behaviors that underlie navigation.

### Keywords

*C. elegans*; feedback; GABA<sub>B</sub> receptor; GPCR; locomotion; muscarinic

### Introduction

Divergence is a widespread and important theme in the biology of signaling: the divergence of one molecule to many receptor classes generates a large repertoire of responses to the release of a single chemical. All known transmitter molecules that mediate fast chemical synaptic transmission via ionotropic receptors also activate a variety of GPCRs thereby extending neurotransmission into multiple intracellular signaling pathways. Ionotropic receptors and GPCRs have very distinct signaling properties. Fast synaptic transmission is mediated by ligand-gated ion channels, which have rapid kinetics (operating on time scales of a few milliseconds), and relatively low affinity for neurotransmitter ligands (typically  $K_D \sim 0.1$ – $1$  mM), which restricts activation to only those receptors that are clustered adjacent to pre-synaptic release sites. These properties endow synapses with the ability to produce the extremely fast, local signals that underlie fast synaptic transmission.

---

Corresponding author with complete address, including an email address: Joshua M Kaplan, Department of Molecular Biology, Massachusetts General Hospital – Simches Research Bldg. 7th Floor, 185 Cambridge St. Boston MA 02114, E-mail: kaplan@molbio.mgh.harvard.edu.

**Jeremy Dittman's current address:** Department of Biochemistry, Weill Cornell Medical College, New York, NY 10021

By contrast, neurotransmitter-gated GPCRs have properties that typically limit their function to slower, modulatory signals. Neurotransmitter-gated GPCRs regulate neuronal activity via a cascade of cytoplasmic second messengers, giving these signals intrinsically slow kinetics (operating on timescales of seconds to minutes), although in some cases, direct binding of the beta gamma subunit can modulate ion channels in tens to hundreds of milliseconds (Dittman and Regehr, 1997). GPCRs have relatively high affinity for neurotransmitter ligands ( $K_D \sim 0.1\text{--}1 \mu\text{M}$ ), which permits activation of receptors that are relatively far-removed from neurotransmitter release sites (Hille, 1992). Thus, signals produced by neurotransmitter-gated GPCRs act over longer timescales, and larger spatial domains.

Although a great deal is known about the contribution of neurotransmitter-gated ion channels to fast synaptic transmission and behavior, much less is known about how neurotransmitter-gated GPCRs regulate circuit activity and behavior. In mammals, extrasynaptic GABA inhibits neuronal activity via metabotropic GABA ( $\text{GABA}_B$ ) receptors (Isaacson et al., 1993; Dittman and Regehr, 1997), whereas extrasynaptic glutamate can both stimulate and inhibit neighboring neurons by activating ionotropic and metabotropic receptors (Mitchell and Silver, 2000; DiGregorio et al., 2002; Szapiro and Barbour, 2007). Thus, the same neurotransmitters that directly gate a postsynaptic ionotropic receptor can influence intracellular signaling in both the pre and postsynaptic cell as well as neighboring neurons.

The nematode *C. elegans* provides a simple model organism for investigating the behavioral impact of neurotransmitter-gated GPCRs. Nematode propulsion arises from sinusoidal waves of muscle contraction and relaxation driven by ACh and GABA respectively (Croll, 1975; Niebur and Erdos, 1993; Schuske et al., 2004). *C. elegans* locomotion is extensively regulated by G protein signaling pathways, including antagonistic regulation of ACh secretion by Go and Gq (Hajdu-Cronin et al., 1999; Lackner et al., 1999; Miller et al., 1999; Nurrish et al., 1999; Robatzek and Thomas, 2000; Robatzek et al., 2001; Bastiani and Mendel, 2006). While these studies suggest that Go and Gq play important roles in regulating locomotion, much less is known about the upstream GPCRs regulating these pathways, and specifically about the role of neurotransmitter-gated GPCRs. In this study, we identified two motor neuron GPCRs that detect ACh and GABA, and analyzed the locomotion behavior of mutants lacking these receptors.

## Materials and Methods

### Strains

Strains were maintained at 20 °C as described by Brenner (Brenner, 1974). The following strains were used in this study: N2 Bristol, *gar-2(ok520)*, *gbb-1(tm1406)*, *gbb-2(tm1165)*, *goa-1(sa734)*, KP3473: *nuIs155 [Punc-17::Venus::GAR-2]*, KP3457: *nuEx1076 [Punc-17::Venus::GAR-3]*, KP3456: *gar-2(ok520);nuEx1075 [Pgar-2::Venus::GAR-2]*, KP3526: *nuEx1072 [Pgar-2::GFP];nuEx1067 [Punc-25::dsRed2]*, KP3447: *nuEx1066 [Pgbb-1::GFP];nuEx1067*, KP4488: *Punc-25::Venus::GAR-2;gar-2(ok520)*, *eri-1(mg366);lin-15B(n744)*.

The *eri-1;lin-15B* strain was used for feeding RNA interference (RNAi) experiments because neurons of wild-type animals are refractory to RNAi. This strain was developed to provide enhanced sensitivity to RNA interference in neurons (Sieburth et al., 2005).

### Constructs and Transgenes

cDNA encoding the splice form GAR-2a was subcloned into the fire lab vector pPD49.26 flanked by NheI and KpnI. An in-frame NotI site was introduced after the start codon and YFP<sub>venus</sub> was ligated to create an N-terminal fusion protein. The signal sequence from *pat-3*

beta integrin was included on the 5' end of YFP-Venus to insure proper receptor insertion. Tissue-specific expression of this fusion protein was determined by including about 3 kb of 5' regulatory sequence from *unc-17* VChT (for all cholinergic neurons), *gar-2* (for rescue construct), or *unc-25* GAD (for rescue in GABAergic neurons only). cDNA encoding the splice form GAR-3b was subcloned as described for GAR-2a. Transcriptional reporters for *gar-2* and *gbb-1* were made by subcloning 3 kb of 5' regulatory sequence for each of these genes into the Fire lab vector pPD95.75 which contains a cDNA encoding soluble GFP. The *unc-25* reporter construct was made by replacing GFP in pPD95.75 with DsRed2 (Clontech) and then subcloning 3 kb of 5' regulatory sequence from the *unc-25* gene.

Predictions for the gene structures of *gbb-1* and *gbb-2* were generated using GeneMark HMM routines (<http://opal.biology.gatech.edu/GeneMark/eukhmm.cgi>), and cDNAs were amplified and sequenced from a *C. elegans* cDNA library. Two splice variants for *gbb-1* were identified: 2.5 and 2.6 kb whereas only one cDNA for *gbb-2* was identified.

### Fluorescence Imaging

Venus::GAR-2 expressing animals were mounted on agarose pads and viewed on a Zeiss Axiovert microscope, using an Olympus PlanApo 100x NA 1.4 objective, as described previously (Dittman and Kaplan, 2006). Images were captured with a Hamamatsu ORCA digital camera and line scans were analyzed with custom software in Igor Pro (Wavemetrics). Images of 500 nm fluorescein-conjugated beads (Molecular Probes) were captured during each imaging session to provide a fluorescence standard for comparing absolute fluorescence levels between animals. Background signal (CCD dark current and slide autofluorescence) was subtracted before analysis.

### Aldicarb and Levamisole Assays

Sensitivity to aldicarb and levamisole was determined by analyzing the onset of paralysis following treatment with either 1 mM aldicarb (Chem Services) or 200  $\mu$ M levamisole (Sigma) as described previously (Nurrish et al., 1999). Each assay included between 2 and 4 plates of at least 20 animals for each genotype being tested. The experimenter was blind to the genotypes. Each genotype was tested between 4 and 10 independent experiments and paralysis curves were generated by averaging paralysis time courses for each plate.

### Worm Tracking and Analysis

For tracking measurements, worms were reared at 20 °C and moved to room temperature 30 minutes prior to imaging. Young adult animals were picked to agar plates with no bacterial lawn (5–15 worms per plate). Imaging began 5–10 minutes after worms were removed from food. One minute digital videos of individual animals were captured at 8x magnification and 4 Hz frame rate on a Zeiss Discovery Stereomicroscope using Axiovision software. If the animal left the field of view, acquisition was paused while the plate was manually recentered and after a few seconds, acquisition was restarted. The center of mass was recorded for each animal on each video frame using object tracking software in Axiovision. The trajectories were then analyzed using custom software written in Igor Pro 5.0 (Wavemetrics). The raw data was filtered to remove artifactual discontinuities in the trajectory due to noise in the center-of-mass estimates. Speed and angle values were calculated and from frame-by-frame changes in position and angle (from  $-180^\circ$  to  $+180^\circ$ ), with turns and reversals estimated as follows: turns were counted as angle changes between  $50^\circ$  and  $160^\circ$  (taking the absolute value of the angle change). Reversals were counted as angle changes between  $170^\circ$  and  $180^\circ$ . The accuracy of these criteria was assessed by visual inspection of the video. Averages for speed, turn number, and reversal number were determined for each animal and then pooled to form estimated values for each genotype. Standard error was based on the animal-to-animal variation in parameter values. Typically between 40 and 70 animals were assayed for each genotype. For  $R_{\max}$

distributions, the maximal Euclidean distance from the starting point within a 40 second time interval was recorded for each animal. The cumulative distributions of Rmax values were compared between genotypes using the Kolmogorov-Smirnov statistic.

### Worm Curvature Analysis

Images were collected for 10 to 15 animals at 20x magnification using a Zeiss Discovery stereomicroscope. The animals selected were on or near the bacterial lawn and relatively stationary. The anterior-posterior axis of the animal was traced by hand in Axiovision and the x-y coordinates of the traced path were recorded and further analyzed using custom written software in Igor Pro 5.0 (Wavemetrics). Data were smoothed to remove extraneous curvature due to the tracing technique and the local curvature of the smoothed trace was calculated according to the parametric equation of curvature:

$$K = \frac{x'y'' - x''y'}{(x'^2 + y'^2)^{3/2}} \text{ where } x' = \frac{dx}{dt}, y' = \frac{dy}{dt}, x'' = \frac{d^2x}{dt^2}, y'' = \frac{d^2y}{dt^2}$$

The average curvature over the length of the animal was then calculated as:  $\sqrt{\sum K^2 / L_{worm}}$  where  $L_{worm}$  is the length of the worm. This measure was averaged for all worms for each genotype and normalized to wild-type average.

## Results

### GAR-2/M2 mediates inhibition of cholinergic neurons when ACh levels are pharmacologically enhanced

The worm genome contains numerous conserved neurotransmitter-gated GPCRs, including three muscarinic acetylcholine receptors (mAChRs), four dopamine (DARs), three serotonin (5-HTRs), two glutamate (mGluRs) receptors, and two predicted GABA<sub>B</sub> receptor subunits (Bargmann, 1998; Lee et al., 2000; Chase et al., 2004; Carre-Pierrat et al., 2006). We examined the effects of neuronal mAChRs on motor neuron function and locomotion using an M2 receptor GAR-2 deletion mutant (*gar-2(ok520)*) and RNA interference. The *ok520* deletion removes 1.1 kb of the gene including most of the third intracellular (i3) loop, a region of the receptor that is essential for coupling to G proteins (Kubo et al., 1988; Burstein et al., 1996), and consequently is likely to eliminate GAR-2 function. ACh levels are normally limited by synaptic AChEs so inhibiting cholinesterase activity will elevate ACh (Hartzell et al., 1975). To experimentally enhance ACh levels, we used the AChE inhibitor aldicarb. Aldicarb treatment induces paralysis with a characteristic time course due to enhanced muscle activation (Miller et al., 1996; Nurrish et al., 1999).

To test the effects of GAR-2 on cholinergic motor neuron synapses, we measured the time course of acute paralysis induced by aldicarb in *gar-2* mutants. The *gar-2* deletion mutation and *gar-2* inactivation by RNAi both accelerated the time course of aldicarb-induced paralysis (Figure 1A and B). Muscle sensitivity to the ionotropic cholinergic agonist levamisole was not altered in the *gar-2* mutant (Figure 1C), indicating that intrinsic muscle sensitivity to ACh was not affected by loss of GAR-2. Wild-type aldicarb sensitivity was restored in *gar-2* mutants by expressing an N-terminal YFP(Venus)-tagged GAR-2 cDNA using the *gar-2* promoter. These results suggest that GAR-2 regulates the activity of ventral cord motor neurons.

GAR-2 has been previously shown to be expressed throughout the nervous system including ventral cord neurons but not in muscle (Lee et al., 2000). Consistent with this study, we found that GAR-2 was expressed in some cholinergic motor neurons as well as GABAergic motor

neurons, the two major types of ventral cord motor neurons (Figure 2A). We examined subcellular localization of GAR-2 by expressing a YFP::GAR-2 fusion protein in cholinergic motor neurons and imaged the dorsal cord (Figure 2Ad). The protein appeared to be diffusely distributed in axons with no obvious spatial relationship to presynaptic terminals. A similar pattern was seen using a C-terminal fusion protein GAR-2::YFP (data not shown).

To determine which motor neurons require GAR-2, we expressed *gar-2* cDNA constructs in subsets of cholinergic or GABAergic motor neurons of *gar-2* mutants (Figure 2B). When GAR-2 was expressed in all cholinergic motor neurons using the vesicular ACh transporter (VACHT) *unc-17* promoter, transgenic animals became strongly resistant to aldicarb (*gar-2(ACh)* Figure 2B). In contrast, no rescue was observed when GAR-2 was expressed in GABAergic motor neurons using the *unc-25* glutamic acid decarboxylase (GAD) promoter (*gar-2(GABA)* Figure 2B). These results suggest that GAR-2 mediates feedback inhibition of cholinergic motor neurons when ACh levels are elevated by aldicarb treatment.

### GOA-1 is required for GAR-2/M2 mediated feedback inhibition

GAR-2 is predicted to be a M2/4 subtype mAChR (36% identity, 60% similarity to rat M2), which couples to the Gai/o class of G proteins (Lanzafame et al., 2003). In animals lacking the G $\alpha$ o subunit GOA-1, aldicarb-induced paralysis is greatly accelerated, consistent with a loss of feedback inhibition by G $\alpha$ o-coupled GPCRs (Figure 2C) (Hajdu-Cronin et al., 1999; Miller et al., 1999; Nurrish et al., 1999). The aldicarb resistance caused by *gar-2(ACh)* was eliminated in *goa-1* mutants (Figure 2C), indicating that GAR-2 inhibition requires G $\alpha$ o.

### Ectopic expression of GAR-3/M3 switches the sign of feedback regulation

Excess GAR-2 in all cholinergic neurons likely exaggerates G $\alpha$ o-mediated inhibition when ACh is increased by aldicarb treatment. By contrast, the G $\alpha$ q pathway enhances transmitter secretion in a variety of systems including cholinergic motor neurons (Hajdu-Cronin et al., 1999; Lackner et al., 1999; Miller et al., 1999; Bauer et al., 2007). We reasoned that we could switch the sign of feedback regulation by ectopically expressing a muscarinic receptor that couples to G $\alpha$ q in cholinergic motor neurons. To test this idea, we ectopically expressed the worm M1/3 type muscarinic receptor (GAR-3) in cholinergic neurons. GAR-3 normally activates the G $\alpha$ q pathway in pharyngeal muscle (Steger and Avery, 2004; You et al., 2006). If GAR-3 activation in cholinergic motor neurons leads to enhanced ACh release, we would expect that the resulting positive feedback would severely disrupt normal locomotion. In contrast, excess GAR-2 expression would be expected to have little effect under conditions where activation by excess ACh is minimal. We monitored the effects of changing muscarinic signaling on body posture as well as aldicarb sensitivity. As a measure of resting motor neuron drive onto body wall muscles, we calculated the curvature along the anterior-posterior (A-P) axis of quiescent animals, where basal curvature is maintained by the steady-state balance of muscle contraction on both sides of the body. The average A-P curvature was unaffected by either removal or overexpression of GAR-2 whereas overexpression of GAR-3 (*gar-3(ACh)*) caused resting curvature to double ( $122 \pm 23$  % increase,  $p < 0.01$ ) (Fig. 3A, B). As a second assay, we compared the time course of paralysis when ACh levels were increased with aldicarb. In contrast to the delayed paralysis observed in *gar-2(ACh)* animals, paralysis was greatly accelerated in *gar-3(ACh)* animals (Figure 3C), further supporting the notion that *gar-3(ACh)* animals are highly sensitive to increases in ambient ACh.

### GABA<sub>B</sub> receptors mediate heterosynaptic feedback when ACh levels are enhanced

During a body bend, ACh depolarizes muscles on one side of the body while GABA release hyperpolarizes the antagonist muscles on the contralateral side (Schuske et al., 2004). GABAergic motor neurons are driven exclusively by excitatory input by cholinergic motor neurons. As a consequence of this connectivity, conditions that enhance ACh release will cause

a parallel increase in GABA release. Thus, in addition to the fast synaptic inhibition of muscle activity by ionotropic GABA receptors, metabotropic GABA receptors may detect elevated GABA levels and produce longer term modulation of neuronal or muscle activity. Consistent with this idea, two genes predicted to encode GABA<sub>B</sub> receptor subunits were identified in a large-scale RNA interference screen for aldicarb hypersensitivity (Vashlishan et al., 2008). *gbb-1* (Y41G9A.4) encodes the worm GABA<sub>B</sub>R1 subunit (40% identity, 63% similarity to rat GBR1) and *gbb-2* (zk180.1/2) encodes the worm GABA<sub>B</sub>R2 subunit (31% identity, 56% similarity to rat GBR2). Knockdown of these two gene products by RNAi accelerated paralysis in aldicarb similar to RNAi of *gar-2* (data not shown).

To confirm these RNAi results, we examined the effects of two deletion mutants that are predicted to eliminate GABA<sub>B</sub> receptor function. The *gbb-1(tm1406)* mutant contains a 1281 base pair deletion that removes the ligand binding site for GABA on the N terminus of the receptor (Fig. 4A) (Bettler et al., 2004). The *gbb-2(tm1165)* mutant contains a 364 base pair deletion that removes transmembrane regions 2, 3, and 4 including the second intracellular (i2) loop which is required for activation G $\alpha$  subunits (Bettler et al., 2004) (Fig. 4A). GABA<sub>B</sub> receptors function as obligate heterodimers where GABA binding is mediated by the GABA<sub>B</sub>R1 subunit and G protein coupling is mediated by the GABA<sub>B</sub>R2 subunit (Bettler et al., 2004); consequently, both deletion alleles are predicted to eliminate GABA<sub>B</sub> receptor function. As shown in Figure 4B, both deletion mutants resulted in nearly identical acceleration of paralysis in aldicarb, similar to loss of GAR-2 receptor function. This hypersensitivity to aldicarb was not likely due to changes in muscle sensitivity to ACh because *gbb-1* and *gbb-2* mutants were not hypersensitive to the cholinergic agonist levamisole (Fig. 4C). We examined interactions between GAR-2, GBB-1, and GBB-2 by measuring paralysis rates in aldicarb for double mutants. The rate of aldicarb-induced paralysis of the *gbb-1;gbb-2* double knockout was indistinguishable from that observed in either single mutant (Fig. 4D), consistent with GBB-1 and GBB-2 functioning together as a heterodimer. However, we found a significant degree of additivity in the *gar-2;gbb-2* double knockout at early time points in the aldicarb paralysis time course (Fig 4D), suggesting that both mAChR and GABA<sub>B</sub> receptors contribute to G $\alpha$ o signaling when ACh is elevated.

A transcriptional reporter containing the *gbb-1* promoter driving expression of GFP was broadly expressed in the nervous system, including cholinergic but not GABAergic motor neurons or muscle (Fig. 4E). Because *gbb-1/2* mutants were hypersensitive to ACh accumulation and had wild-type levamisole sensitivity, cholinergic expression of GABA<sub>B</sub> receptors suggests that they detect GABA released from neighboring GABAergic motor neurons. These GABAergic neurons predominantly form synapses onto muscle so the GABA that activates cholinergic GABA<sub>B</sub> receptors is probably extrasynaptic in origin.

### Feedback regulation by muscarinic and GABA<sub>B</sub> receptors regulates locomotion

Thus far, our results implicate GAR-2 and GBB-1/2 in the regulation of cholinergic motor neuron function when levels of ACh and GABA are increased by aldicarb treatment. To determine whether this feedback inhibition normally plays a role in locomotion, we analyzed the movement of actively foraging animals in the absence of aldicarb. Figure 5A shows representative trajectories of wild type, *gar-2* mutant, *gar-2(ACh)*, and *gar-3(ACh)* worms over a one minute interval. These trajectories followed the center of mass for each animal as it explored an agar plate. Wild-type and *gar-2* mutants had similar patterns of exploratory behavior consisting of long runs of forward locomotion interrupted by brief reversals and large-angle turns as has been described previously (Pierce-Shimomura et al., 1999; Hills et al., 2004). In contrast, *gar-2(ACh)* and *gar-3(ACh)* animals showed aberrant trajectories and explored a more restricted area in a given time interval. We quantified locomotory behavior using three parameters: speed, turning frequency, and reversal frequency. Speed of locomotion

was slightly but significantly accelerated in *gar-2* mutants ( $9.2 \pm 3.1$  % increase,  $p < 0.01$ ) and retarded in *gar-2(ACh)* animals ( $25.4 \pm 2.7$  % decrease,  $p < 0.01$ ) suggesting that GAR-2 regulates the speed of locomotion (Fig. 5B). When GAR-3 was ectopically expressed in cholinergic motor neurons, the locomotory speed was greatly reduced ( $74.6 \pm 3.4$  % decrease,  $p < 0.01$ ).

In addition to GAR-2 receptor effects on speed, direction changes were also subject to GAR-2 regulation. Turning frequency was defined as the number of large-angle (between  $50^\circ$  and  $160^\circ$ ) forward turns per minute, while reversals were scored as  $180^\circ \pm 10^\circ$  changes in direction. Removal of GAR-2 decreased the frequency of turns in half ( $60.8 \pm 8.3$  % decrease,  $p < 0.01$ ) whereas excess GAR-2 did not affect turning frequency (Fig. 5C). Ectopic expression of GAR-3 however, dramatically increased the turning rate ( $\sim 8$  fold increase,  $p < 0.01$ ) to such an extent that animals coiled back on themselves and were unable to maintain forward progress (see Fig. 3A image). The rate of reversals was also reduced by half in *gar-2* mutants ( $52.5 \pm 8.7$  % decrease,  $p < 0.01$ ) whereas excess GAR-2 doubled the reversal rate ( $103.1 \pm 28.3$  % increase,  $p < 0.01$ ) and ectopic GAR-3 caused a modest increase ( $45.9 \pm 23.5$  %,  $p < 0.05$ ) (Fig. 5D). The maximum net distance an animal could travel in a given time interval is determined by the speed as well as turning and reversal rates. We calculated this maximum distance ( $R_{\max}$ ) as a measure of the net velocity of an animal over an extended period of time. A schematic of the maximal distance measure is shown in Figure 5E. Within a 40 second interval, the most distant point from the starting location ( $R_{\max}$ ) was determined for each animal and a cumulative histogram of  $R_{\max}$  was generated. The median distance reached by wild-type animals ( $n=67$ ) was about 3.5 mm whereas *gar-2* mutants ( $n=72$ ) reached a median distance of 4.3 mm, corresponding to a 25% increase ( $p < 0.01$ ) in the net distance covered by *gar-2* mutants (Fig 5F). All effects on locomotory behavior could be rescued by Venus::GAR-2 expression under the endogenous promoter (*rescue*, Fig. 5). Thus, GAR-2 regulates how often animals change direction and the extent of the area they explore in a given time.

We next analyzed the role of GABA<sub>B</sub> receptors in regulating locomotion. The effects of removing GABA<sub>B</sub> receptor modulation on locomotion were similar to those observed in *gar-2* mutants (Fig. 6). Speed was accelerated significantly ( $20 \pm 3.5$  % increase,  $p < 0.01$ ) whereas turn and reversal frequency were decreased ( $41.4 \pm 10.1$  % and  $42.5 \pm 13.4$  % respectively,  $p < 0.05$ ). The maximal distance covered in 40 seconds was significantly increased in both double knockouts (wild type median = 3.5 mm, *gar-2;gbb-2* median = 4.1 mm, *gbb-1;gbb-2* median = 4.4 mm). In contrast to the additivity observed in the time course of aldicarb paralysis, no additivity was observed on locomotory changes. Thus, the same receptors that provide negative feedback under conditions of elevated transmitter also regulate locomotory behavior. The observations described above suggest that ACh and GABA released during normal foraging behavior modulate aspects of locomotion and navigation, in addition to their roles in fast excitatory and inhibitory transmission.

## Discussion

Here we use *C. elegans* as a model to identify two neuronal GPCRs that detect transmitter ligands, and to test their impact on a behavioral circuit. First, we identify GAR-2/M2 and GBB-1/2 GABA<sub>B</sub>R as the GPCRs that detect ACh and GABA, respectively, in the ventral cord. The M2 receptor, GAR-2 is expressed in motor neurons and mediates negative feedback via the G $\alpha$  pathway during periods of increased ACh release. Second, *C. elegans* employs a GABA<sub>B</sub> receptor dimer in cholinergic motor neurons that mediates heterosynaptic inhibition, likely through the G $\alpha$  pathway. Third, both GAR-2/M2 and GABA<sub>B</sub> receptors promote initiation of direction changes during locomotion. Ectopic expression of GAR-2 in all cholinergic neurons bestows profound negative feedback when ACh levels are elevated, and transgenic animals exhibit opposite locomotory phenotypes as loss of GAR-2 including slower

speed and greater frequency of reversals. Finally, adding positive feedback through ectopic expression of the  $G\alpha_q$ -coupled muscarinic receptor GAR-3/M3 severely disrupts locomotion by promoting exaggerated body bends.

### Site of Action: Synaptic versus Extrasynaptic activation of GAR-2 and GBB-1/2

In this study, we found that cholinergic motor neurons expressed muscarinic and  $GABA_B$  receptors. In principle, these receptors could be strictly localized to postsynaptic sites in which case, the behavioral effects described here were due to disruption of a select group of synaptic inputs with a major postsynaptic metabotropic component. Alternatively, these receptors could be acting as detectors of extrasynaptic ACh and GABA accumulating through ongoing synaptic activity. We favor the latter possibility for several reasons. First, the affinity and signaling kinetics of metabotropic receptors are not suited to the rapid spikes of neurotransmitter concentration that peak at hundreds of micromolar to millimolar levels and decay within milliseconds. In contrast, neurotransmitter levels can increase above the micromolar level outside of the synaptic cleft via spillover and summate when multiple synapses are concurrently active (Isaacson et al., 1993; Dittman and Regehr, 1997; DiGregorio et al., 2002). This extrasynaptic source of neurotransmitter would take significantly longer to clear below micromolar levels due to the larger volume (Carter and Regehr, 2000; DiGregorio et al., 2002), making it ideal for activation of slow, high affinity receptors.

Second, when subcellular localization of metabotropic receptors has been studied using immunoelectron microscopy and fluorescently tagged GPCRs, there is often a significant population of perisynaptic and nonsynaptic receptors (Liu et al., 1998; Fritschy et al., 1999). We did not observe enrichment of GAR-2 within neuronal processes nor did GAR-2 appear to be excluded from synaptic regions further suggesting that these receptors are not strictly localized. Furthermore, given the high affinity of GAR-2 receptors for ACh, receptors found at the synapse would be expected to be constitutively liganded and desensitized by the high local concentrations of ACh achieved in the synaptic cleft.

Third, many GPCRs detect neurotransmitter that is not synaptically released onto the neurons in which they are expressed. For instance,  $GABA_B$  receptors are commonly found near presynaptic terminals of glutamatergic neurons that do not receive direct axo-axonal synapses from GABAergic interneurons in the hippocampus and cerebellum. Cholinergic motor neurons expressed the GBB-1  $GABA_B$  receptor subunit even though no GABAergic to cholinergic neuron synapses have been described in *C. elegans* (White et al., 1976). Indeed, cholinergic neurons also express dopamine receptors even though they do not receive direct dopaminergic inputs (Chase et al., 2004). For these reasons, we postulate that GAR-2 and GBB-1/2 act to inhibit cholinergic activity in response to increases in ambient extrasynaptic ACh and GABA.

### Conservation of Muscarinic and $GABA_B$ Receptors in nematodes

Presynaptic M2 muscarinic receptors are known to modulate synaptic transmission at both NMJs and central synapses in mammals by signaling through  $G\alpha_o$  (Haddad el and Rousell, 1998; Gomez et al., 1999; Zhang et al., 2007). Conservation of this pathway in nematodes suggests that GAR-2 participates in an ancient negative modulatory axis to regulate neuronal function.

$GABA_B$  receptor subunits have been predicted by sequence homology after sequencing of the worm genome (Duthey et al., 2002). Here, we confirm that *C. elegans* expresses two gene products that share a high degree of homology to vertebrate  $GABA_B$  receptors both in the GABA-binding domain and the heptahelical transmembrane region. In vertebrates,  $GABA_B$  receptors are heterodimers made up of a  $GABA_B R1$  subunit that binds GABA and a  $GABA_B R2$  subunit that binds the C terminus of  $G\alpha_o$  through its i2 loop (Duthey et al., 2002;

Bettler et al., 2004; Thuault et al., 2004). Interestingly, the GABA<sub>B</sub>R1 subunit GBB-1 GABA-binding domain has substantially greater amino acid sequence identity with its rodent ortholog than GBB-2 compared to rodent GABA<sub>B</sub>R2 (55% vs 31%, Fig 4A), whereas GBB-2 shares higher amino acid identity with its ortholog in the heptahelical region, especially in the i2 loop (58% vs 25% for GBB-2 and GBB-1 respectively). Thus, phylogenetic conservation of these domains reflects their function in GABA binding and G $\alpha$  signaling.

### Determinants of locomotory behaviors in *C. elegans*

Neurotransmitter-activated GPCRs have been implicated in many functions of the mammalian sensory and motor systems. For instance, rodent knockouts of M2 and GABA<sub>B</sub>R subunits have been associated with specific locomotory alterations (Gomez et al., 1999; Schuler et al., 2001; Zhang et al., 2002; Gassmann et al., 2004). *C. elegans* possesses simple sensory and motor circuits that are amenable to precise genetic changes in GPCR function. These nematodes navigate their environment through long runs of forward locomotion interrupted by brief reversals and large-angle (omega turn) body bends that alter direction (Croll, 1975). Many of the neurons that initiate or control these stereotyped behaviors have been identified (Pierce-Shimomura et al., 1999; Hills et al., 2004; Gray et al., 2005). Because loss of either GAR-2 or GBB-1/2 decreases reversal and omega turn frequencies, and over-expression of GAR-2 increases reversal frequency, it is possible that these inhibitory receptors act in neurons that normally suppress turns and reversals. The gustatory sensory neuron ASI, the interneuron AIY, as well as a head motor neuron, RIM have all been reported to inhibit reversals and omega turns (Gray et al., 2005). Thus, these neurons would be candidates for targets of inhibitory GPCR modulation. RIM in particular is cholinergic and therefore may employ homosynaptic negative feedback to regulate its suppression of reversals. Further studies elaborating on the specific neurons that endogenously express GAR-2 will reveal how ACh signaling in the navigation circuits use GAR-2 to trigger direction changes.

GPCRs generally modulate neuronal activity on a time scale of hundreds of milliseconds to many seconds. Since the body bends that drive locomotion occur at a rate of about one per second, it is unlikely that transmitter release and activation of GAR-2 and GBB-1/GBB-2 will modulate locomotion within a body bend. Instead, these pathways may set the basal tone of inhibition. In addition, the GPCR mutant data suggest that the transition between behaviors (i.e. reversal of direction) may itself be modulated. These transitions occur at a frequency of 1 to 5 per minute so there is ample time for neurotransmitter to accumulate and activate the G $\alpha$  pathway.

### An *in vivo* analysis of feedback regulation

Neurotransmitter spillover has been proposed to mediate homo- and hetero-synaptic depression and, consequently, to play an important role in activity dependent modulation of circuit function (Dittman and Regehr, 1997; Mitchell and Silver, 2000). Here we describe a possible role for extrasynaptic ACh and GABA in regulating a locomotory circuit via metabotropic receptors. In particular, we focused on a negative feedback loop created by the inhibitory action of ACh and GABA on cholinergic neurons. Negative feedback typically provides a stabilizing force that can contribute to the fine tuning of a network. Exchanging a negative feedback loop for a positive feedback would likely abolish this stability since small perturbations would be greatly amplified. In the case of exchanging an M2 receptor for an M3 receptor, small increases in extrasynaptic ACh would now drive further ACh release by coupling to a stimulatory pathway. Even under resting conditions, transgenic animals expressing the M3 receptor showed severe dysfunction of coordinated locomotion. Body bend angles were greatly increased, compromising the ability of the animal to generate and propagate the sinusoidal waves necessary for normal locomotion.

In addition to the homosynaptic negative feedback provided by cholinergic GAR-2 receptors, GABA MNs also expressed GAR-2. Although GABAergic rescue of GAR-2 did not restore wild-type aldicarb sensitivity, it is possible that heterosynaptic effects of ACh on GABA neurons may be important for navigational behaviors.

Our results extend *C. elegans* as a genetic model to dissect the functional impact of GPCR-mediated feedback regulation on a behavioral circuit. Future studies will help elucidate the particular neurons involved in modulating locomotory behavior as well as the spatial and temporal domains over which the GAR-2 and GBB-1/2 receptors sense their ligands and modulate the nervous system.

## Acknowledgements

This work was supported by a research grant (GM54728) from the National Institutes of Health (J.K.) and by a Damon Runyon CRF postdoctoral fellowship (J.D.). We thank the *C. elegans* Genetic Stock Center and S. Mitani for strains. We also thank members of the Kaplan lab for comments on this manuscript.

## References

- Bargmann CI. Neurobiology of the *Caenorhabditis elegans* genome. *Science* 1998;282:2028–2033. [PubMed: 9851919]
- Bastiani, C.; Mendel, J. *WormBook*. 2006. Heterotrimeric G proteins in *C. elegans*; p. 1-25.
- Bauer CS, Woolley RJ, Teschemacher AG, Seward EP. Potentiation of exocytosis by phospholipase C-coupled G-protein-coupled receptors requires the priming protein Munc13-1. *J Neurosci* 2007;27:212–219. [PubMed: 17202488]
- Bettler B, Kaupmann K, Mosbacher J, Gassmann M. Molecular structure and physiological functions of GABA(B) receptors. *Physiol Rev* 2004;84:835–867. [PubMed: 15269338]
- Brenner S. The genetics of *Caenorhabditis elegans*. *Genetics* 1974;77:71–94. [PubMed: 4366476]
- Burstein ES, Spalding TA, Brann MR. Constitutive activation of chimeric m2/m5 muscarinic receptors and delineation of G-protein coupling selectivity domains. *Biochem Pharmacol* 1996;51:539–544. [PubMed: 8619900]
- Carre-Pierrat M, Baillie D, Johnsen R, Hyde R, Hart A, Granger L, Segalat L. Characterization of the *Caenorhabditis elegans* G protein-coupled serotonin receptors. *Invert Neurosci* 2006;6:189–205. [PubMed: 17082916]
- Carter AG, Regehr WG. Prolonged synaptic currents and glutamate spillover at the parallel fiber to stellate cell synapse. *J Neurosci* 2000;20:4423–4434. [PubMed: 10844011]
- Chase DL, Pepper JS, Koelle MR. Mechanism of extrasynaptic dopamine signaling in *Caenorhabditis elegans*. *Nat Neurosci* 2004;7:1096–1103. [PubMed: 15378064]
- Croll NA. Behavioural analysis of nematode movement. *Adv Parasitol* 1975;13:71–122. [PubMed: 1169872]
- DiGregorio DA, Nusser Z, Silver RA. Spillover of glutamate onto synaptic AMPA receptors enhances fast transmission at a cerebellar synapse. *Neuron* 2002;35:521–533. [PubMed: 12165473]
- Dittman JS, Regehr WG. Mechanism and kinetics of heterosynaptic depression at a cerebellar synapse. *J Neurosci* 1997;17:9048–9059. [PubMed: 9364051]
- Dittman JS, Kaplan JM. Factors regulating the abundance and localization of synaptobrevin in the plasma membrane. *Proc Natl Acad Sci U S A* 2006;103:11399–11404. [PubMed: 16844789]
- Duthey B, Caudron S, Perroy J, Bettler B, Fagni L, Pin JP, Prezeau L. A single subunit (GB2) is required for G-protein activation by the heterodimeric GABA(B) receptor. *J Biol Chem* 2002;277:3236–3241. [PubMed: 11711539]
- Fritschy JM, Meskenaite V, Weinmann O, Honer M, Benke D, Mohler H. GABAB-receptor splice variants GB1a and GB1b in rat brain: developmental regulation, cellular distribution and extrasynaptic localization. *Eur J Neurosci* 1999;11:761–768. [PubMed: 10103070]
- Gassmann M, Shaban H, Vigot R, Sansig G, Haller C, Barbieri S, Humeau Y, Schuler V, Muller M, Kinzel B, Klebs K, Schmutz M, Froestl W, Heid J, Kelly PH, Gentry C, Jaton AL, Van der Putten

- H, Mombereau C, Lecourtier L, Mosbacher J, Cryan JF, Fritschy JM, Luthi A, Kaupmann K, Bettler B. Redistribution of GABAB(1) protein and atypical GABAB responses in GABAB(2)-deficient mice. *J Neurosci* 2004;24:6086–6097. [PubMed: 15240800]
- Gomez J, Shannon H, Kostenis E, Felder C, Zhang L, Brodtkin J, Grinberg A, Sheng H, Wess J. Pronounced pharmacologic deficits in M2 muscarinic acetylcholine receptor knockout mice. *Proc Natl Acad Sci U S A* 1999;96:1692–1697. [PubMed: 9990086]
- Gray JM, Hill JJ, Bargmann CI. A circuit for navigation in *Caenorhabditis elegans*. *Proc Natl Acad Sci U S A* 2005;102:3184–3191. [PubMed: 15689400]
- Haddad el B, Rousell J. Regulation of the expression and function of the M2 muscarinic receptor. *Trends Pharmacol Sci* 1998;19:322–327. [PubMed: 9745360]
- Hajdu-Cronin YM, Chen WJ, Patikoglou G, Koelle MR, Sternberg PW. Antagonism between G(o)alpha and G(q)alpha in *Caenorhabditis elegans*: the RGS protein EAT-16 is necessary for G(o)alpha signaling and regulates G(q)alpha activity. *Genes Dev* 1999;13:1780–1793. [PubMed: 10421631]
- Hartzell HC, Kuffler SW, Yoshikami D. Post-synaptic potentiation: interaction between quanta of acetylcholine at the skeletal neuromuscular synapse. *J Physiol* 1975;251:427–463. [PubMed: 171379]
- Hille B. G protein-coupled mechanisms and nervous signaling. *Neuron* 1992;9:187–195. [PubMed: 1353972]
- Hills T, Brockie PJ, Maricq AV. Dopamine and glutamate control area-restricted search behavior in *Caenorhabditis elegans*. *J Neurosci* 2004;24:1217–1225. [PubMed: 14762140]
- Isaacson JS, Solis JM, Nicoll RA. Local and diffuse synaptic actions of GABA in the hippocampus. *Neuron* 1993;10:165–175. [PubMed: 7679913]
- Kubo T, Bujo H, Akiba I, Nakai J, Mishina M, Numa S. Location of a region of the muscarinic acetylcholine receptor involved in selective effector coupling. *FEBS Lett* 1988;241:119–125. [PubMed: 3197827]
- Lackner MR, Nurrish SJ, Kaplan JM. Facilitation of synaptic transmission by EGL-30 Gqalpha and EGL-8 PLCbeta: DAG binding to UNC-13 is required to stimulate acetylcholine release. *Neuron* 1999;24:335–346. [PubMed: 10571228]
- Lanzafame AA, Christopoulos A, Mitchelson F. Cellular signaling mechanisms for muscarinic acetylcholine receptors. *Receptors Channels* 2003;9:241–260. [PubMed: 12893537]
- Lee YS, Park YS, Nam S, Suh SJ, Lee J, Kaang BK, Cho NJ. Characterization of GAR-2, a novel G protein-linked acetylcholine receptor from *Caenorhabditis elegans*. *J Neurochem* 2000;75:1800–1809. [PubMed: 11032868]
- Liu XB, Munoz A, Jones EG. Changes in subcellular localization of metabotropic glutamate receptor subtypes during postnatal development of mouse thalamus. *J Comp Neurol* 1998;395:450–465. [PubMed: 9619499]
- Miller KG, Emerson MD, Rand JB. Galpha and diacylglycerol kinase negatively regulate the Gqalpha pathway in *C. elegans*. *Neuron* 1999;24:323–333. [PubMed: 10571227]
- Miller KG, Alfonso A, Nguyen M, Crowell JA, Johnson CD, Rand JB. A genetic selection for *Caenorhabditis elegans* synaptic transmission mutants. *Proc Natl Acad Sci U S A* 1996;93:12593–12598. [PubMed: 8901627]
- Mitchell SJ, Silver RA. Glutamate spillover suppresses inhibition by activating presynaptic mGluRs. *Nature* 2000;404:498–502. [PubMed: 10761918]
- Niebur E, Erdos P. Theory of the locomotion of nematodes: control of the somatic motor neurons by interneurons. *Math Biosci* 1993;118:51–82. [PubMed: 8260760]
- Nurrish S, Segalat L, Kaplan JM. Serotonin inhibition of synaptic transmission: Galpha(0) decreases the abundance of UNC-13 at release sites. *Neuron* 1999;24:231–242. [PubMed: 10677040]
- Pierce-Shimomura JT, Morse TM, Lockery SR. The fundamental role of pirouettes in *Caenorhabditis elegans* chemotaxis. *J Neurosci* 1999;19:9557–9569. [PubMed: 10531458]
- Robatzek M, Thomas JH. Calcium/calmodulin-dependent protein kinase II regulates *Caenorhabditis elegans* locomotion in concert with a G(o)/G(q) signaling network. *Genetics* 2000;156:1069–1082. [PubMed: 11063685]

- Robatzek M, Niacaris T, Steger K, Avery L, Thomas JH. eat-11 encodes GPB-2, a Gbeta(5) ortholog that interacts with G(o)alpha and G(q)alpha to regulate *C. elegans* behavior. *Curr Biol* 2001;11:288–293. [PubMed: 11250160]
- Schuler V, Luscher C, Blanchet C, Klix N, Sansig G, Klebs K, Schmutz M, Heid J, Gentry C, Urban L, Fox A, Spooren W, Jatou AL, Vigouret J, Pozza M, Kelly PH, Mosbacher J, Froestl W, Kaslin E, Korn R, Bischoff S, Kaupmann K, van der Putten H, Bettler B. Epilepsy, hyperalgesia, impaired memory, and loss of pre- and postsynaptic GABA(B) responses in mice lacking GABA(B(1)). *Neuron* 2001;31:47–58. [PubMed: 11498050]
- Schuske K, Beg AA, Jorgensen EM. The GABA nervous system in *C. elegans*. *Trends Neurosci* 2004;27:407–414. [PubMed: 15219740]
- Sieburth D, Ch'ng Q, Dybbs M, Tavazoie M, Kennedy S, Wang D, Dupuy D, Rual JF, Hill DE, Vidal M, Ruvkun G, Kaplan JM. Systematic analysis of genes required for synapse structure and function. *Nature* 2005;436:510–517. [PubMed: 16049479]
- Steger KA, Avery L. The GAR-3 muscarinic receptor cooperates with calcium signals to regulate muscle contraction in the *Caenorhabditis elegans* pharynx. *Genetics* 2004;167:633–643. [PubMed: 15238517]
- Szapiro G, Barbour B. Multiple climbing fibers signal to molecular layer interneurons exclusively via glutamate spillover. *Nat Neurosci* 2007;10:735–742. [PubMed: 17515900]
- Thuault SJ, Brown JT, Sheardown SA, Jourdain S, Fairfax B, Spencer JP, Restituito S, Nation JH, Topps S, Medhurst AD, Randall AD, Couve A, Moss SJ, Collingridge GL, Pangalos MN, Davies CH, Calver AR. The GABA(B2) subunit is critical for the trafficking and function of native GABA(B) receptors. *Biochem Pharmacol* 2004;68:1655–1666. [PubMed: 15451409]
- Vashlishan AB, Madison JM, Dybbs M, Bai J, Sieburth D, Ch'ng Q, Tavazoie M, Kaplan JM. An RNAi Screen Identifies Genes that Regulate GABA Synapses. *Neuron* 2008;58:346–361. [PubMed: 18466746]
- White JG, Southgate E, Thomson JN, Brenner S. The structure of the ventral nerve cord of *Caenorhabditis elegans*. *Philos Trans R Soc Lond B Biol Sci* 1976;275:327–348. [PubMed: 8806]
- You YJ, Kim J, Cobb M, Avery L. Starvation activates MAP kinase through the muscarinic acetylcholine pathway in *Caenorhabditis elegans* pharynx. *Cell Metab* 2006;3:237–245. [PubMed: 16581001]
- Zhang HM, Chen SR, Pan HL. Regulation of glutamate release from primary afferents and interneurons in the spinal cord by muscarinic receptor subtypes. *J Neurophysiol* 2007;97:102–109. [PubMed: 17050831]
- Zhang W, Basile AS, Gomeza J, Volpicelli LA, Levey AI, Wess J. Characterization of central inhibitory muscarinic autoreceptors by the use of muscarinic acetylcholine receptor knock-out mice. *J Neurosci* 2002;22:1709–1717. [PubMed: 11880500]

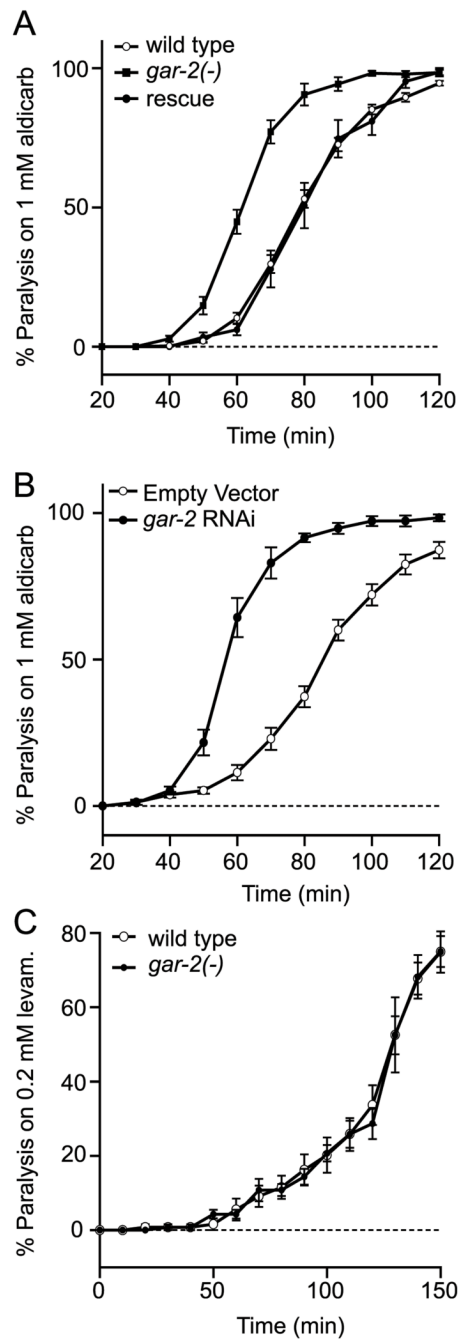


**Figure 1.**

*gar-2* mutant animals are hypersensitive to the cholinesterase inhibitor, aldicarb. A. Paralysis time course in 1 mM aldicarb for wild type (open circles), *gar-2* (closed squares), and cDNA rescue (closed circles). B. Paralysis time course in 1 mM aldicarb for the enhanced RNAi strain *eri-1;lin-15B* (see Methods). Animals were fed empty vector (open circles) or *gar-2* RNA vector (closed squares). C. Paralysis time course in 0.2 mM levamisole for wild type (open circles) and *gar-2* (closed circles). Data are mean  $\pm$  SEM.

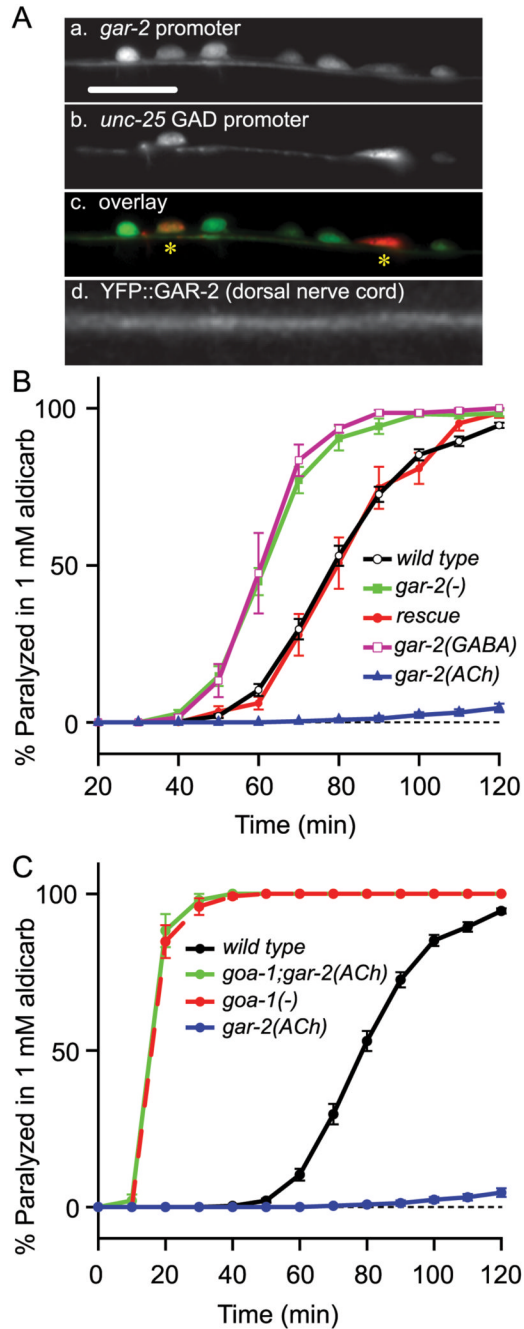
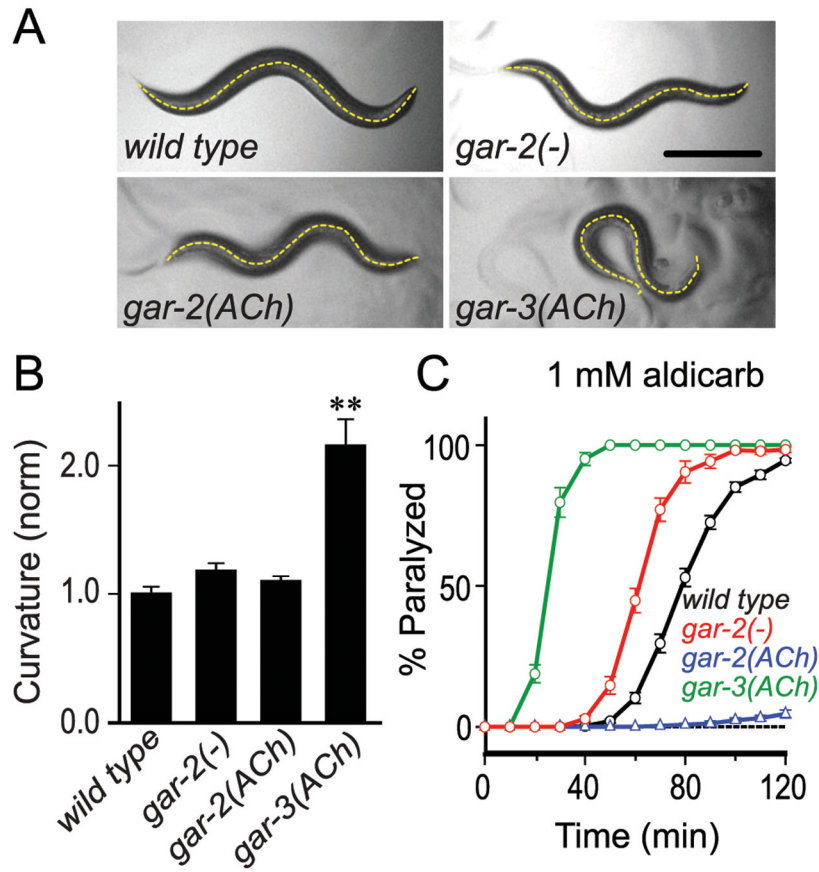


**Figure 2.**

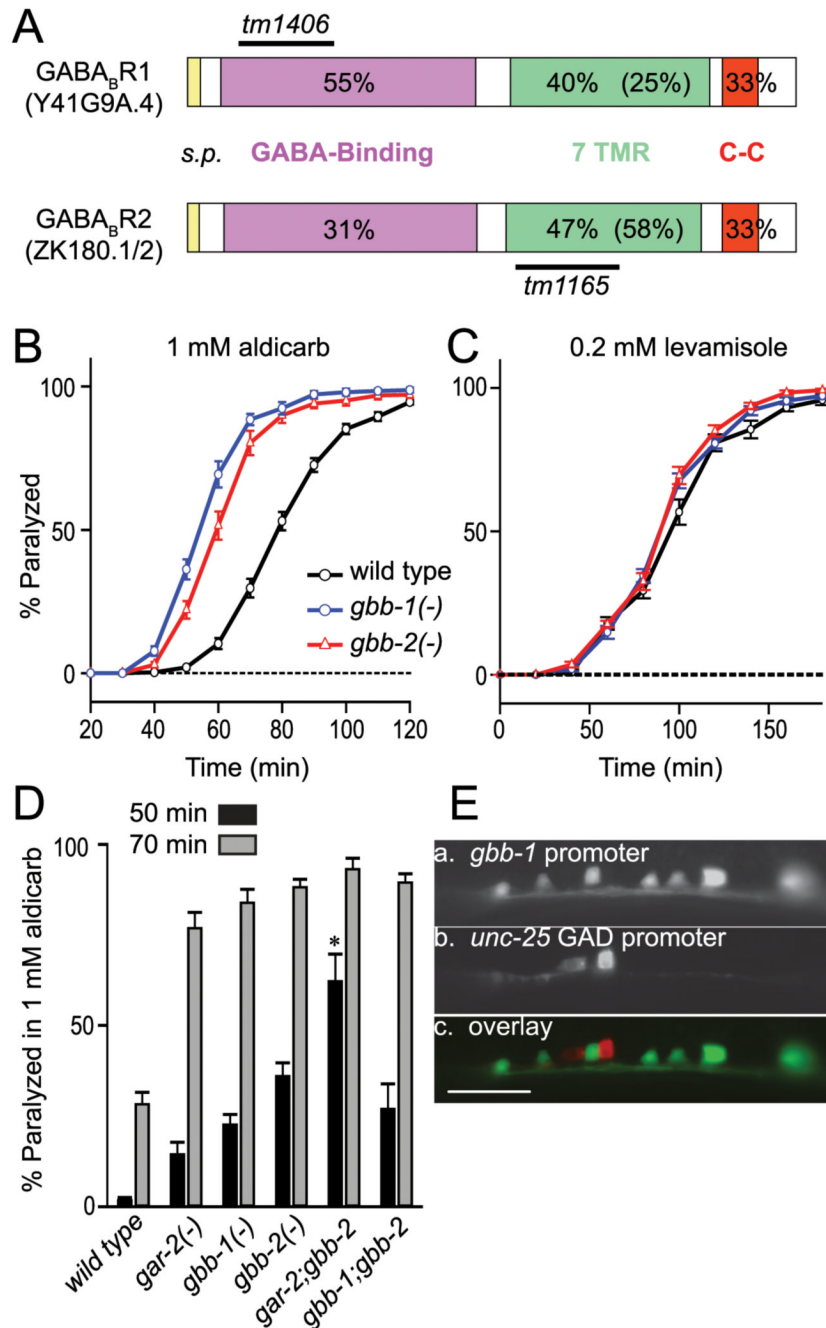
GAR-2/M2 is expressed in cholinergic and GABAergic motor neurons and requires *goa-1* Gαo. A. Representative image of ventral cord motor neurons expressing soluble GFP driven by the *gar-2* promoter (a) and soluble DsRed2 driven by the *unc-25* GAD promoter (b). The two images are superimposed to illustrate neurons that coexpress GFP and DsRed2 (c). Asterisks mark GABA motor neurons expressing GAR-2. YFP<sub>venus</sub>::GAR-2 expression in a dorsal motor axon (d). Scale bar is 10 microns in a–c and 3.3 microns in d. B. Paralysis time course in 1 mM aldicarb for wild type (open black circles), *gar-2* (closed green squares), *rescue*: cDNA rescue under the *gar-2* promoter (closed red circles), *gar-2*(GABA): cDNA rescue under the *unc-25* GAD promoter (open purple squares), and *gar-2*(ACh): cDNA rescue

under the *unc-25* GAD promoter (open purple squares), and *gar-2*(ACh): cDNA rescue under the *unc-25* GAD promoter (open purple squares), and *gar-2*(ACh): cDNA rescue under the *unc-25* GAD promoter (open purple squares). C. Paralysis time course in 1 mM aldicarb for wild type (open black circles), *goa-1*;*gar-2*(ACh) (closed green squares), *goa-1*(-) (closed red circles), and *gar-2*(ACh) (closed blue triangles). Error bars represent standard deviation.

under the *unc-17* VAcHT promoter (*closed blue triangles*). C. Paralysis time course in 1 mM aldicarb for wild type (*closed black circles*), *goa-1G $\alpha$*  (*closed red circles*), *gar-2(ACh)*: cDNA rescue under the *unc-17* VAcHT promoter (*closed blue circles*), and *goa-1;gar-2(ACh)* (*closed green circles*). Data are mean  $\pm$  SEM.

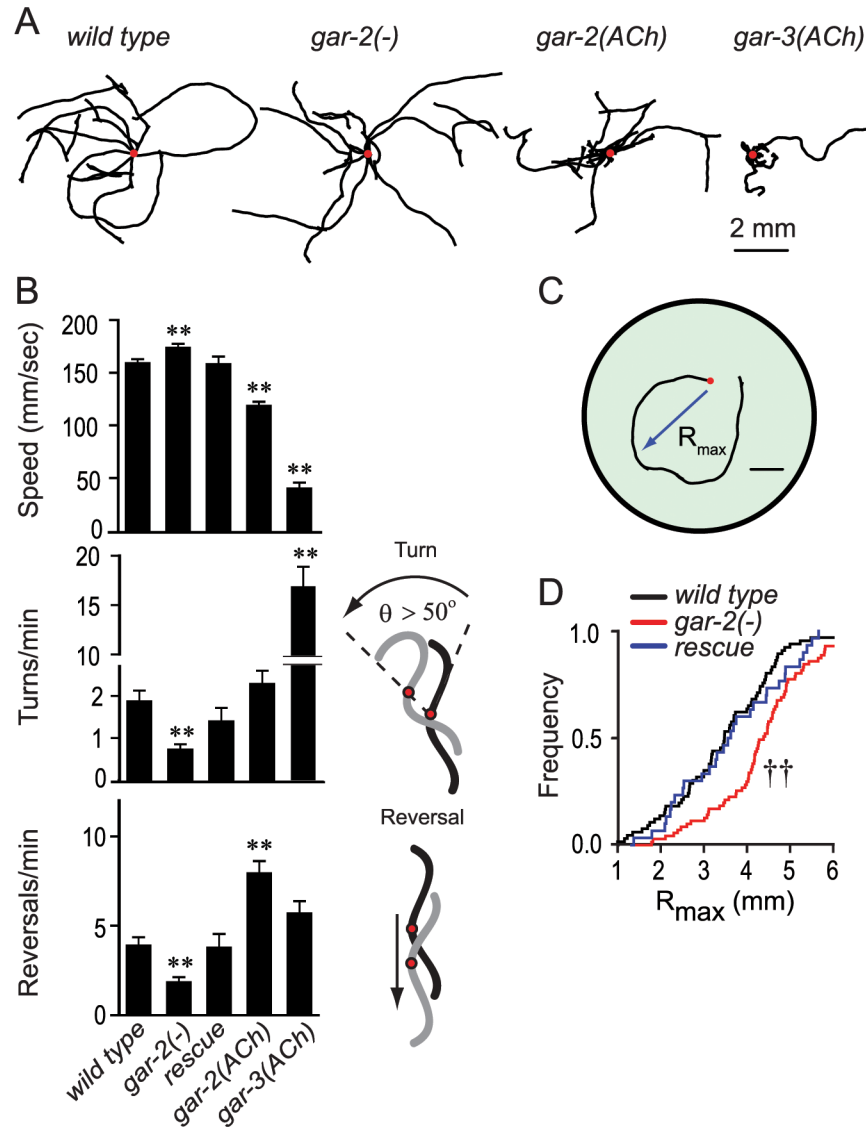


**Figure 3.** Ectopic GAR-3 mAChR3 in cholinergic motor neurons enhances ACh release. **A.** Representative images of wild type, *gar-2* mutant, *gar-2(ACh)*, and *gar-3(ACh)* animals with overlaid trace of anterior-posterior (A-P) axis used for measuring body posture curvature. Scale bar is 300 microns. **B.** A-P curvature averaged over length of animal for the 4 genotypes shown above (see Methods for calculation of curvature). \*\*  $p < 0.01$  by Student's T test. **C.** Paralysis time course in 1 mM aldicarb for wild type (black), *gar-2* (red), *gar-2(ACh)*: cDNA rescue under the *unc-17* VAcHT promoter (blue), and *gar-3(ACh)*: *gar-3* mAChR3 cDNA expression under the *unc-17* VAcHT promoter (green). Data are mean  $\pm$  SEM.

**Figure 4.**

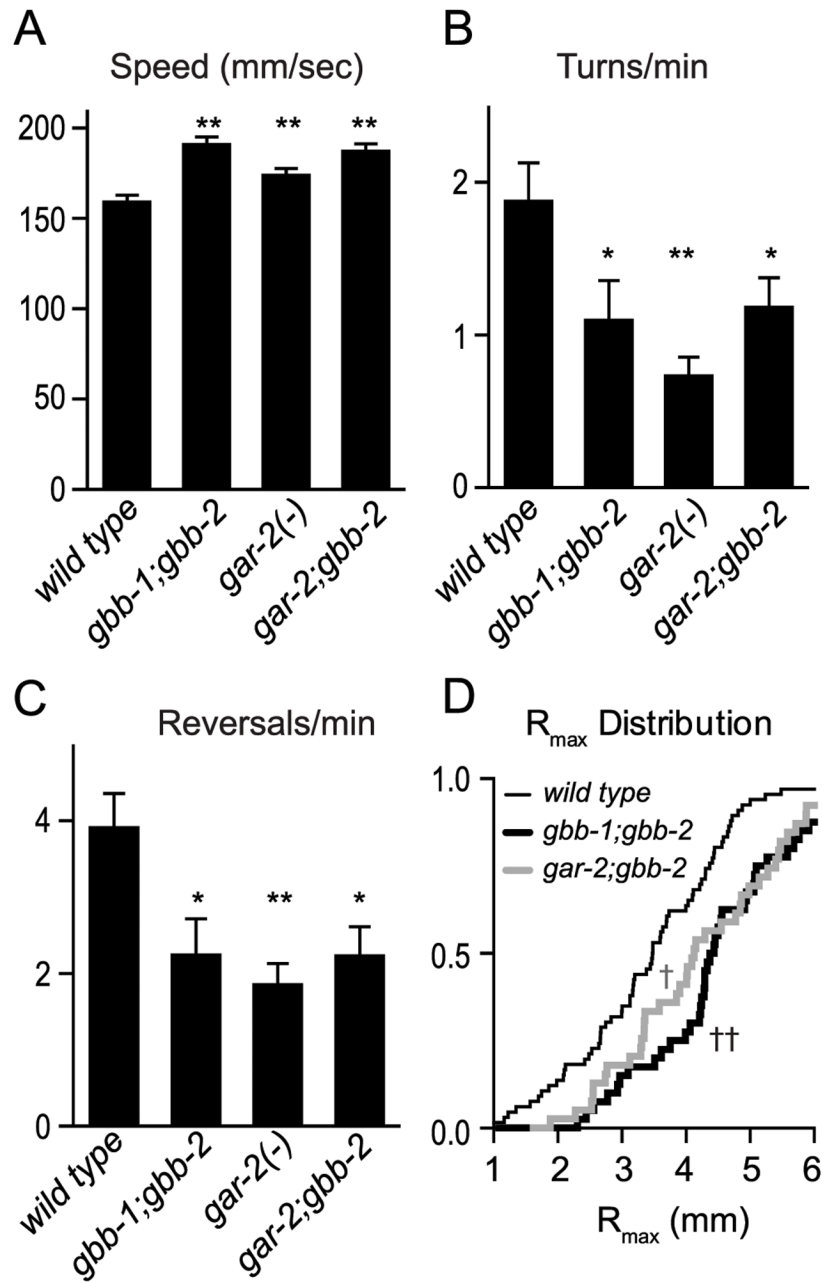
GABA<sub>B</sub> receptor mutants are hypersensitive to aldicarb. A. Protein domain structure for GBB-1 and GBB-2. Domains indicated are signal peptide (*s.p.*), amino acid binding domain (*GABA-Binding*), heptahelical transmembrane region (*7 TMR*), and coiled-coil domain (*C-C*). Percentages are amino acid sequence identity to orthologous rat GABA<sub>B</sub> receptor domains. Parenthetical percentages are amino acid identity within the second intracellular (i2) loop. Deletions for knockout alleles are indicated. Paralysis time course in 1 mM aldicarb (B), and 0.2 mM levamisole (C) for wild type (*open black circles*), *gbb-1* (*open blue circles*), and *gbb-2* (*open red triangles*). D. Percentage of animals paralyzed on 1 mM aldicarb at 50 minutes (*black*) and 70 minutes (*gray*) for wild type, single and double mutants as indicated. E.

Representative image of ventral cord motor neurons expressing soluble GFP driven by the *gbb-1* promoter (*a*) and soluble DsRed2 driven by a GABAergic neuron-specific promoter (*b*). The two images are superimposed to illustrate neurons do not coexpress GFP and DsRed2 (*c*). Scale bar is 5 microns. Data are mean  $\pm$  SEM. \*\*  $p < 0.01$  compared to *gar-2*, *gbb-1*, and *gbb-2* by Student's T test.



**Figure 5.**

Effects of Muscarinic Receptors on locomotion. **A**. Representative trajectories superimposed for 10 animals of each genotype as indicated. The starting points for each of the trajectories were aligned for clarity (*red circles*). **B**. Average frame-to-frame speed of the center-of-mass in microns per second for the genotypes shown above as well as *gar-2* cDNA rescue. **C**. Average frequency of large-angle forward turns defined as angles greater than  $50^\circ$  but less than  $160^\circ$ . **D**. Average frequency of direction reversals defined as angles near  $180^\circ$ . **E**. Cartoon showing the trajectory of an animal during a 40 second interval. The maximal Euclidean distance from the starting point (*red circle*) is defined as  $R_{\max}$ . Scale bar is 1 mm. **F**. Cumulative distributions of  $R_{\max}$  during a 40 second interval for wild type (*black*), *gar-2* mutant (*red*), and cDNA rescue (*blue*). Data are mean  $\pm$  SEM. \*\*  $p < 0.01$  by Student's T test. ††  $p < 0.01$  by Kolmogorov-Smirnov.

**Figure 6.**

GABA<sub>B</sub> receptors modulate locomotion. Center-of-mass speed (A), large-angle turn frequency (B), and reversal frequency (C) for wild type, *gbb-1;gbb-2* double KO, *gar-2*, and *gar-2;gbb-2* double KO animals. D. Cumulative distributions of R<sub>max</sub> for wild type (thin line), *gbb-1;gbb-2* double KO (thick black line), and *gar-2;gbb-2* double KO (thick gray line). Data are mean ± SEM. \*\* p < 0.01, \* p < 0.05 compared to wild type by Student's T test. †† p < 0.01, † p < 0.05 by Kolmogorov-Smirnov.